Proceeding of the
XVth Bi-Annual Symposium on Measuring Techniques in
Transonic and Supersonic Flows in Cascades and Turbomachines
21-22 September, Firenze/Italy

GLUE-ON HOT FILM SENSORS TO INVESTIGATE HEAT TRANSFER ON A HIGHLY LOADED LP FILM COOLED TURBINE BLADE

Stefan Wolff, Leonhard Fottner
Institut für Strahlantriebe
Universität der Bundeswehr München
D-85577 Neubiberg, Germany
Stefan.Wolff@unibw-muenchen.de

ABSTRACT

This paper describes an attempt to determine heat transfer coefficients using glue-on hot film sensors operated in CTA mode. The anemometer output voltage and the set-up data for the CTA bridge were used to calculate the forced convective heat flux between the heated sensor and the fluid flow.

Often heat transfer coefficients are determined by optical measurement techniques. Due to the fact that e.g. a film cooled leading edge shows a strong curvature, a system would be needed where no optical access is necessary. Therefore the well established hot-film anemometry based on the heat transfer was employed to develop a system to determine quantitative heat transfer coefficients. The results were compared to TLC measurements on the same set-up.

Even though the results showed discrepancies to the TLC heat transfer coefficients most of the phenomena in the vicinity of the film cooling hole were detected. However, further investigations like a measurement without any film cooling hole have to be performed to solve some problems which were outlined.

NOMENCLATURE

Latin

a	[-]	overheat ratio
A	[m^2]	cross-sectional area
b	[m]	gauge width
d	[-]	incremental displacement
D	[m]	hole diameter
E	[V]	voltage
h	[W/(m^{2}K)]	heat transfer coefficient
I	[A]	electrical current
l	[m]	chord length
m	[K$/\Omega$]	gradient of gauge resistance temperature sensitivity
M	[-]	blowing ratio
P	[W]	power, CTA output
$\dot{Q}$	[W]	heat flux
R	[W]	resistance
s	[m]	surface length, s=0 at injection location
T	[K]	temperature
x	[m]	bi-tangential streamwise co-ordinate

Subscripts

0	zero-flow conditions
1, 2	inlet / exit
1..n	indexing number
2th	exit presuming isentropic expansion
c	conductive, property of unheated gauge
C	cooling (secondary) air
cs	cable and support
e	electric
fc	forced convective
G	main flow
H	film cooling hole
L 1;2	leads
P	probe
r	radiation
s	storage
t	total / stagnation
w	property of heated gauge

Abbreviations

CTA	Constant Temperature Anemometry
TLC	Thermocromic Liquid Crystal
HGK	High-Speed Cascade Wind Tunnel

INTRODUCTION

Due to the demands for more efficient gas turbines, turbine inlet temperature increased rapidly in the past enabled by an extensive use of film cooling technology. Therefore a lot of research work was conducted within this area, since improvement in material development did not keep up with the thermal requirements. The review by Goldstein [1] delineates much of the physics of film cooling, especially the jet in cross flow behaviour. In film cooling literature a manifold number of parameters have been investigated with regard to aerodynamic as well as to thermal aspects.

At the beginning of the eighties work focused on the development of reliable methods for the investigations of heat transfer with liquid crystal technology. Hippensteele et al. [2] presented methods for the examination of the heat transfer coefficient using the liquid crystal technique based on the steady state solution of the heat transfer equation. Composites of carbon-films or gold-films were used as electrical heater elements. Tests were conducted on small turbine guide vanes in a plane speed cascade wind tunnel. Camci et al. [3] intensified the studies on the evaluation methods and influence parameters of colour image processing methods for the liquid crystal technique.

Intensive studies at the University of Oxford (e.g. Wang et al. [4]) dealt with a heat transfer evaluation method based on the transient solution of the differential equation. Investigations on the heat transfer at the entrance of inclined film cooling holes were performed by Gillespie et al. [5] on simple geometries. Gritsch et al. [6] and Baldauf et al. [7] used an infrared image processing system.

Other examinations on film cooling were based on the naphthalene sublimation technique (heat-mass transfer analogy) (e.g. Goldstein et al. [8]) or the ammonia and diazo technique (e.g. Haslinger and Hennecke [9]).

Various sensor types were used to determine steady and unsteady heat transfer coefficients with the advantage that no optical access was needed. High-speed heat flux and temperature sensors were used by Popp et al. [10] and thin film gauges were employed by e.g. Hilditch et al. [11] and Sieverding et al. [12].

The present work is an attempt to determine heat transfer coefficients by glue-on hot-films operated in CTA mode, seeing that hot-film anemometry as well as the TLC technique (cf. Ganzert [13]) are based on the convective heat transfer of a heated wall and the ambient fluid flow. The motivation is to provide a measurement technique which does not need optical access and provides the possibility to handle a strong curvature of the surface as it is found at the leading edge.

Several aspects have to be considered using multi sensor arrays. Haselbach [14] dealt with the thermal conduction into the wall and the thermal interaction between two or more heated gauges. Tiedemann [15] introduced a method to calculate the wall temperature distribution from hot-film data. Heselhaus [16] conducted coupled calculations on film cooling problems and discussed the influence of a local temperature step on the heat transfer coefficient.

By using MTU glue-on hot-film gauges on the suction side of a film cooled turbine blade, the measurement technique presented in this paper will be validated. The results will be compared to TLC results on the same test facility. The additional information from the hot film data will help to understand flow phenomena in the near hole region.

EXPERIMENTAL APPARATUS

Turbine cascade

All experimental investigations were performed on a large scale plane cascade turbine model named T106-300. The cascade consists of three blades with 300 mm chord length and two adjustable tailboards at half pitch distance from the upper and lower blade thus assuring flow periodicity and high spatial resolution together with a two dimensional flow field at mid span. For the simulation of film cooling a single row of holes is located on the suction side at 40% chord length. They are connected to large plena in the center of the blades where secondary film cooling air is fed from both sides to the plena. Measurements were carried out exclusively on the center blade. A sectional sketch and the main aerodynamic and geometric data is given in Fig. 1. The film cooling design data is given in Tab. 1.

Chord Length:	300 mm
Blade Height:	300 mm
Pitch Ratio:	0.799
Stagger Angle:	59.28°
Ma_1	0.28
Ma_{2th}	0.59
Re_{2th}	500000
β_1	127.70°
β_2	26.70°
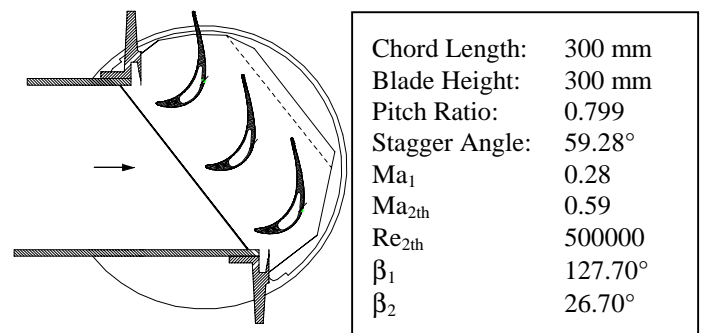
Fig. 1 HGK test section with T106-300 cascade

Film Cooling Position	x/l	0.40
Hole Diameter	D	3.0 mm
Length / Diameter	l_H /D	5
Hole Spacing	t_H	7.5 mm
No. of Holes	n_H	34
Axial hole inclination angle	γ_{Ax}	50°
Lateral hole inclination angle	γ_{Lat}	0°

Tab. 1. Film cooling design data

High-Speed Cascade Wind Tunnel

The experiments were carried out at the High-Speed Cascade Wind Tunnel of the Universität der Bundeswehr München (Fig. 2). This wind tunnel is an open loop facility which can operate continuously and reach Mach numbers up to Ma = 1.05 in the test section. Being built inside a large pressurised tank the wind tunnel offers the possibility to vary independently the Mach and the Reynolds number in order to simulate flow conditions which are typical in modern gas turbines. The total temperature in the settling chamber is set to 303 K as well as the secondary cooling air in order to obtain isothermal conditions. The turbulence intensity can be adjusted by a turbulence generator upstream of the nozzle. For the present study a turbulence level of 3.9% in the test section was detected. A detailed description of the facility is given in Sturm and Fottner [17].

Main test section data:	
Mach Number:	$0.2 \leq Ma \leq 1.05$
Reynolds Number:	$0.2 \cdot 10^6 \, m^{-1} \leq Re/L \leq 16.0 \cdot 10^6 \, m^{-1}$
Inlet Turbulence Level:	$0.4\% \leq Tu_1 \leq 7.5\%$
Inlet Flow Angle:	$25° \leq \beta_1 \leq 155°$
Test Section Width:	300 mm
Test Section Height:	235 mm ... 500 mm

Fig. 2 **High-Speed Cascade Wind Tunnel**

Data acquisition system

The hot-film anemometry technique is often employed to investigate boundary layer development. The present work is an attempt to use glue-on hot-films to obtain heat transfer coefficients. Therefore the well established hot-film data acquisition system (Fig. 3) (Brunner et al. [18]) was adapted and employed. The centre blade of the cascade has been instrumented with an array of 52 MTU hot-film gauges which where embedded (glued on) into the suction side surface. The gauges are located from 12.5 D upstream up to 30 D downstream of the injection location. The centres of the gauges are placed on the centreline of the film cooling holes and cover a hole diameter.

Two racks of the *DANTEC Streamline* anemometer system, each consisting of 6 anemometers, have been employed. Therefore simultaneous data acquisition of 12 hot-film gauges has been possible. A 12 bit A/D board acquires up to 16 channels simultaneously. The set-up data for each gauge is stored in a project file and is available for further evaluation.

Fig. 3 **Layout of the data acquisition system**

Hot-film anemometry

The hot-film anemometry (HFA) as well as the hot-wire anemometry (HWA) is based on the convective heat transfer from the heated sensing element placed in a fluid flow.

Fig. 4 **Heat-rate balance of a glue-on hot-film sensor**

The forced convective heat flux $\dot{Q}_{fc}$ can be determined from the heat-rate balance (Fig. 4) equation (cf. Bruun [19]) for an incremental heated film element:

$$d\dot{Q}_e = d\dot{Q}_{fc} + d\dot{Q}_c + d\dot{Q}_r + d\dot{Q}_s \qquad (1)$$

In order to eliminate the terms of radiation, conductive and storage heat flux, a measurement is conducted under zero flow conditions at the same overheat ratio:

$$d\dot{Q}_{e;0} = d\dot{Q}_{fc;0} + d\dot{Q}_{c;0} + d\dot{Q}_{r;0} + d\dot{Q}_{s;0} \qquad (2)$$

Consider that:

$$d\dot{Q}_{fc;0} = 0$$
$$d\dot{Q}_{c;0} = d\dot{Q}_c \; ; \; d\dot{Q}_{r;0} = d\dot{Q}_r \; ; \; d\dot{Q}_{s;0} = d\dot{Q}_s \qquad (3)$$

The forced convective heat flux is determined as:

$$d\dot{Q}_{fc} = d\dot{Q}_e - d\dot{Q}_{e;0} \qquad (4)$$

The forced convective heat flux can be expressed as well in terms of the heat transfer coefficient h:

$$d\dot{Q}_{fc} = h\, b\, (T_w - T_c)\, dx \qquad (5)$$

Assuming that h is constant, $\dot{Q}_{fc}$ results in:

$$\dot{Q}_{fc} = h\, A\, (T_w - T_c) \qquad (6)$$

The heat generation rate by an electrical current of the hot-film is:

$$\dot{Q}_e = I\, R_w = \frac{E_w^2}{R_w} \qquad (7)$$
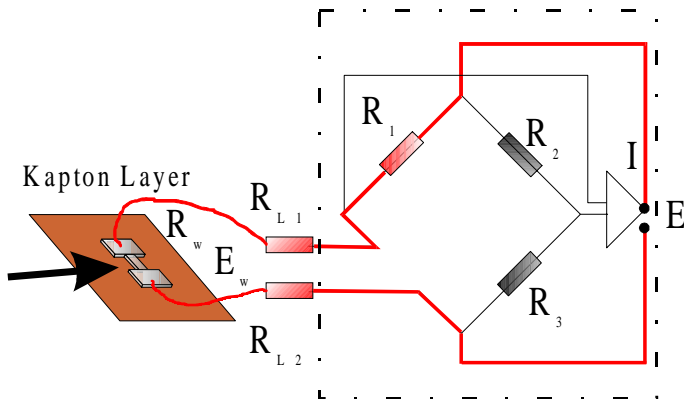
Fig. 5 **Schematic of CTA Wheatstone bridge with hot-film**

The voltage drop over the gauge can be determined by the Kirchhoff´s laws for the electric cycle of the gauge arm shown in Fig. 5:

$$E_w = \frac{R_w}{R_1 + R_{L1} + R_w + R_{L2}} E \qquad (8)$$

where E is the bridge output voltage.

The fixed resistance R_1 and the bridge ratio BR=R_2/R_1 is given by the vendor of the anemometer system. To determine the leads resistance of the connecting from the gauges to the CTA input R_{L1} and R_{L2}, one of the gauges is connected with two leads on both connecting flags. This electric cycle can be used as a shorting probe.

However, it is not possible to measure the resistance of the heated gauge R_w under operating conditions. Nevertheless, the resistance can be determined considering the bridge set-up procedure:
1. Measuring the cold resistance of the probe R_P at Tc
2. Calculating the cold resistance of the gauge by subtracting the resistance of the connecting wires

$$R_c = R_P - R_{L1} - R_{L2} \qquad (9)$$

3. Calculating the hot resistance of the gauge by setting the overheat ratio a:

$$R_w = (1+a)\, R_c \qquad (10)$$

4. Calculating the overheat resistance of the probe

$$R_{P,w} = R_w + R_{L1} + R_{L2} \qquad (11)$$

5. Setting the decade resistance R_3 of the adjust arm of the bridge by the bridge ratio BR:

$$R_3 = BR\, R_{P,w} \qquad (12)$$

For CTA mode R_w is kept constant when the bridge is in balance. The same set-up procedure is done for the zero flow measurement.

Using equation 4, 6 and 7 the heat transfer coefficient h can be calculated as:

$$h = \left(\frac{U_w^2}{R_{w,h}} - \frac{U_{w,0}^2}{R_{w,0,h}} \right) \frac{1}{A(T_w - T_c)} \qquad (13)$$
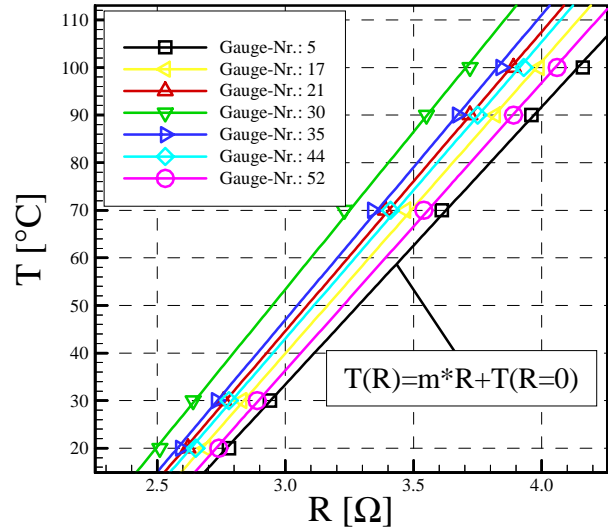
Fig. 6 **Typical examples of hot-film resistance vs. temperature curves**

The temperature difference between the heated and the cold gauge under flow conditions can be determined by calibrating the temperature sensitivity of the gauge resistance. Therefore the instrumented blade was subjected to five different temperatures and the resistance of each gauge was measured and tabled. Examples of calibration curves are shown in Fig. 6.

Related to this calibration measurement the overheat temperature of the gauge can be calculated as:

$$\Delta T = T_w - T_c = m\,(R_w - R_c) = m\,(1+a)\, R_c \qquad (14)$$

4

EXPERIMENTAL RESULTS

In order to provide the same aerodynamic boundary conditions as for the TLC measurements done by Ganzert [13] the profile pressure distribution has been determined by static pressure taps.

Blade Loading

The detected isentropic Mach number distribution (Fig. 7) on the suction side shows a very good agreement with the results presented by Ganzert [13]. For the present studies the pressure taps at $0.25 \leq x/l \leq 0.75$ have to be removed for the hot-film instrumentation.
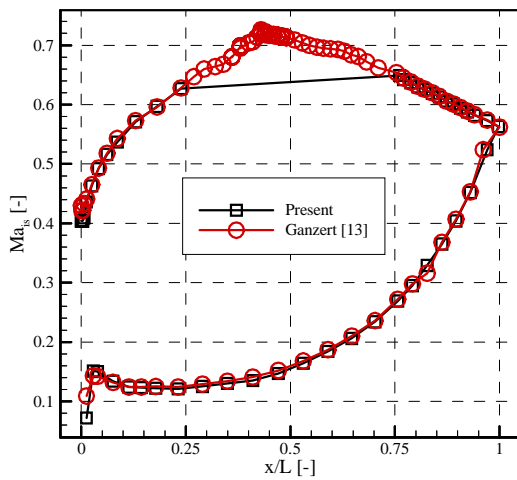
Fig. 7 **Isentropic Mach number distribution**

Hot-Film Data

For a better understanding of the aerodynamics the quasi wall shear stresses as well as the RMS values and the Skewness are calculated from the hot-film data. The quasi wall shear stresses (Fig. 8) are influenced by the blowing ratio in the immediate vicinity of the injection location (s/d=0).

Upstream of the injection the quasi wall shear stresses are decreasing because of decreasing velocity when the boundary layer is decelerated by the film cooling jet for M>0.0.

Downstream of the injection the behavior differs significantly by varying the blowing ratios. At s/D>10 the influence of the blowing ratio is negligible.

The RMS values and the skewness are shown in Fig. 9 and Fig. 10. The transition point for M=0.0 as well as for M=0.5 and 1.0 has been detected at s/D≈6. For M=2.0 no explicit transition point can be determined.
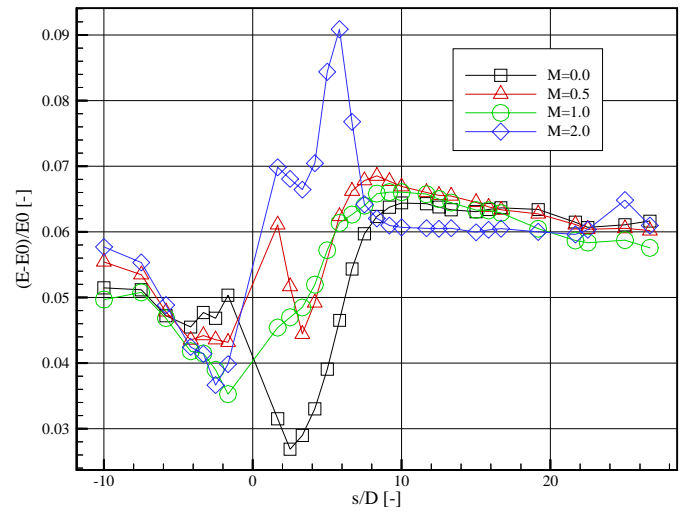
Fig. 8 **Quasi wall shear stresses (M=0.0-2.0)**
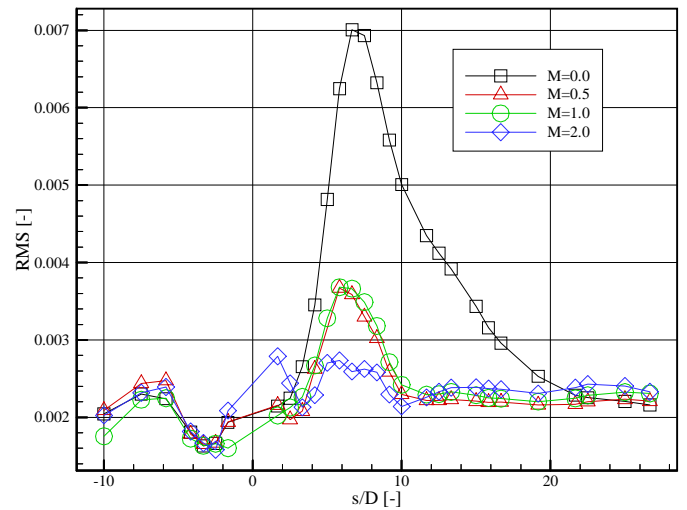
Fig. 9 **RMS Values (M=0.0-2.0)**
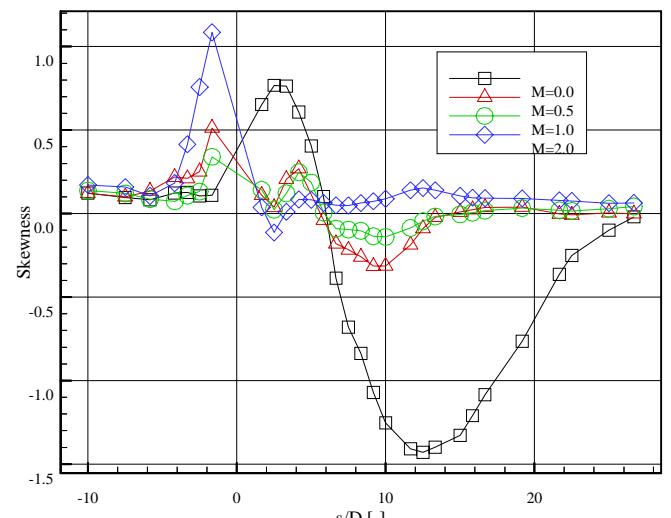
Fig. 10 **Skewness (M=0.0-2.0)**

Heat transfer results

Besides the driving temperature, the effective area of heat exchange has to be determined in order to calculate the heat transfer coefficient. Pictures of a heated gauge with an infrared camera system were taken and evaluated with an image processing system. For the overheat temperature $\Delta T=60K$ a factor of about 4 was determined. But the determination of the effective area of heat exchange between the heated gauge and the fluid flow is identified as a factor of uncertainty. This have to taken into account when evaluating the quantities of the heat transfer coefficient. Using an image processing with a higher spatial resolution will help to reduce the error.

The results calculated with this area are shown in Fig. 11. For all blowing ratios the heat transfer coefficient is decreasing upstream of the injection location where the flow is decelerated by the cooling jet. In the vicinity of the jet in cross flow a massive influence of the blowing ratio is visible. For M=0.0 the heat transfer coefficient drops down downstream of the injection location with a minimum at s/D=2 before it increases to a high constant level at s/D>10.

The blowing ratio M=0.5 shows a local maximum just downstream of the injection and decreases to a local minimum before increasing to the constant level for s/D>10. This behavior was also detected by the TLC measurement.

The heat transfer coefficient for M=1.0 increases continuously from the minimum upstream of the injection to the final value. For the highest momentum M=2.0 the heat transfer coefficient increases rapidly passing the injection and a second peak is detectable at s/D≈6 maybe caused by the reattachment of the jet. Further downstream the heat transfer coefficient drops down to a constant value as well as for the other blowing ratios. Further downstream of S/D=10 no significant influence of the blowing ratio could be detected.

In order to get a better information about the influence of the blowing ratio, the heat transfer coefficient was referenced by the results for M=0.0 (Fig. 12). The ratio decreases for all blowing ratios upstream of the injection. Just downstream of the injection the values shoot up.

The referenced heat transfer coefficient of M=0.5 drops directly to a ratio of 1.5 and decreases more moderately to 1 at s/D=10. More or less all ratios are equal to 1 at s/D>10.

The worst case is given for M=2.0. The ratio is detected to be bigger than 2 up to 6 D with a second peak which may be caused by the reattachment of the film cooling jet.

Comparison with TLC Measurement

First of all it should be noted that the measurements for M=0.0 using the TLC technique were conducted on a blade without any holes. This measurement has also been carried out with the hot-film technique, but due to a software problem during the measurements these results were not used.

The TLC measurements (Fig. 13) as well as the hot-film results show a decreasing upstream and a strong increasing downstream of the injection. It should be noted that the values

of the TLC measurement in the vicinity of a hole are problematical because of the finite distance between the heating meander and the hole. The TLC results show just one peak and a rapid decrease to a lower value than upstream of the injection. The hot-film results level off (s/D>10) at a higher heat transfer coefficient as upstream of the injection. For M=0.5 both measurements detected a double peak at s/D=2 and S/D=6.
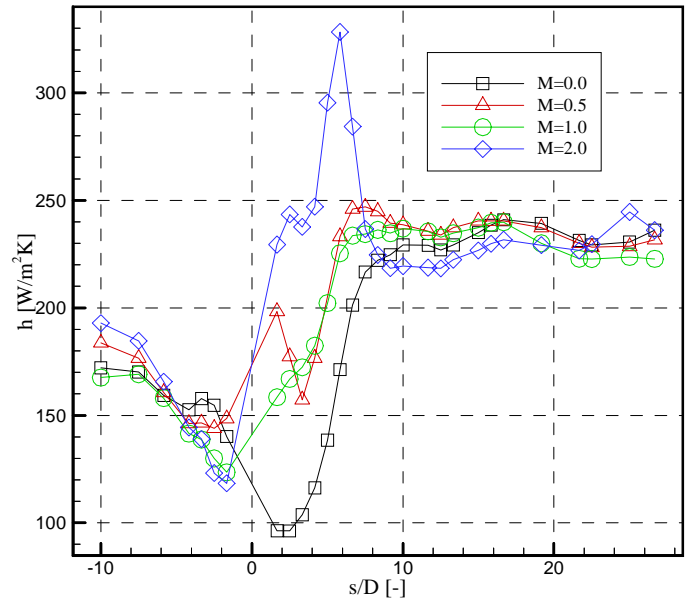
Fig. 11 Heat transfer coefficient ($\Delta T=T_w-T_c$)
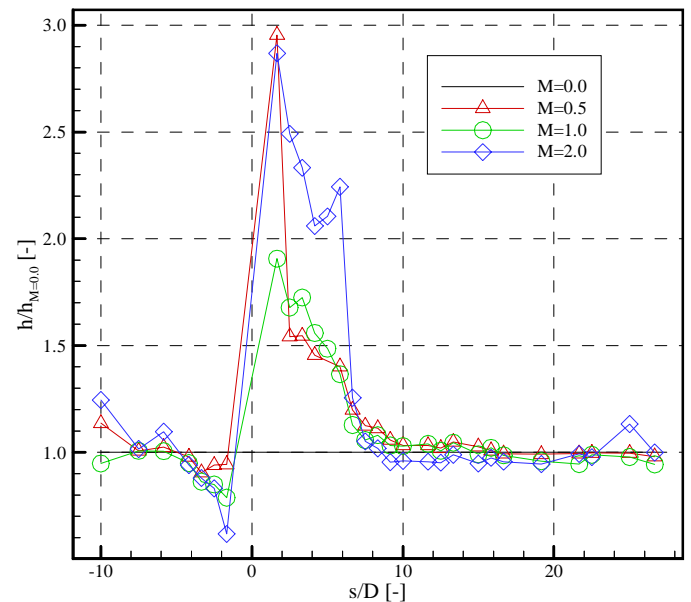
Fig. 12 Heat transfer coefficient referenced by M=0.0 ($\Delta T=T_w-T_c$)

Especially the distribution for M=0.0 is detected totally different. The TLC measurement shows a continuous decreasing heat transfer coefficient downstream of the injection to a level

which is much lower than for the cases with M>0. Also the hot-film results shows a decreasing downstream of the injection (0≤s/D≤3) but further downstream an increasing to the same level as for the other cases can be observed. This high level for the hot film measurement can be explained by the transition of the boundary layer detected by the hot-film results (Fig. 9, Fig. 10) triggered by the film cooling holes.

Due to differences between the results for M=0.0 the values referenced by M=0.0 (Fig. 12, Fig. 14) are on different levels downstream of s/D=10. But there are some interesting phenomena which where detected by both measurement techniques. For M=2.0 a high peak can be found at s/D=2 and a second peak at s/D=6. For M=1.0 the second smaller peak is located at s/D=4.
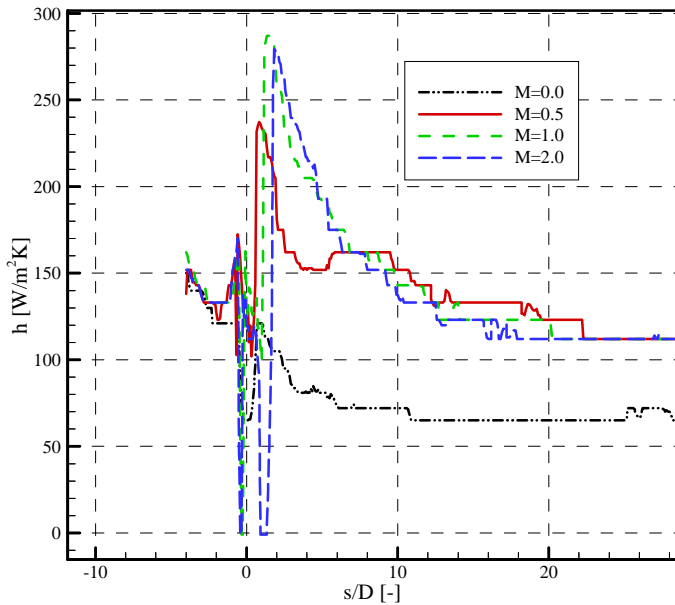
Fig. 13 Heat transfer coefficient (TLC, Ganzert [13])

Comparison to flat plate results

Baldauf et al. [7] conducted an investigation on a flat plat facility with an infrared camera and a cooled wall. The inclination angle was 60° and the density ratio was set to 1.2. In order to compare these results (Fig. 16) the referenced values for the current study where calculated with a driving temperature of $\Delta T = T_w - T_{t,G}$ (Fig. 15). It should be noted that the flat plat results are reasonable downstream of x/D=2 due to the fact that the cooled area of the wall start at this position. The referenced values in Fig. 16 increase further downstream but as well as the hot-film results the increase in heat transfer coefficient downstream of x/D>10 is about 5 to 20%.

CONCLUSION

A method for determination of heat transfer coefficients based on glue-on hot-film measurements was presented. The system to measure heat transfer coefficients with hot-film gauges in CTA mode has been developed to investigate heat transfer effects without the necessity of an optical access. An MTU hot-film array was embedded into the surface on the centerline of a film cooled turbine blade. The combined computer controlled CTA system and a data acquisition system previously used for steady and unsteady hot-film investigations was adapted for the heat transfer investigation.
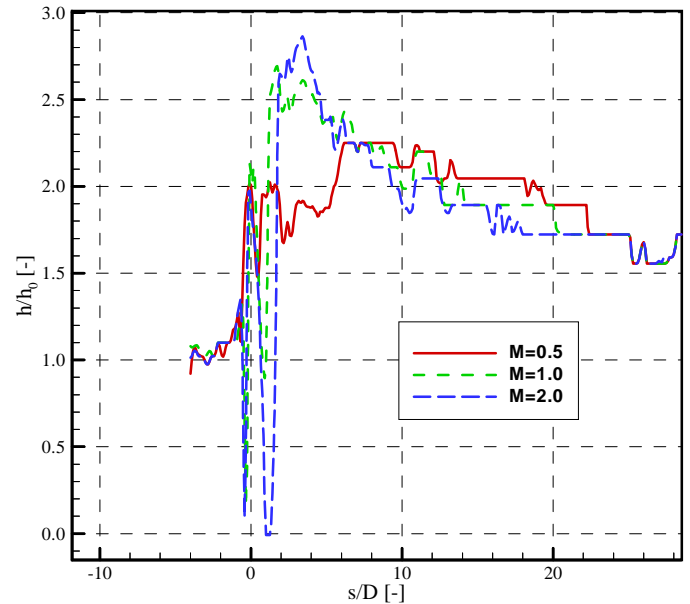
Fig. 14 Heat transfer coefficient referenced by M=0.0 (TLC, Ganzert [1])
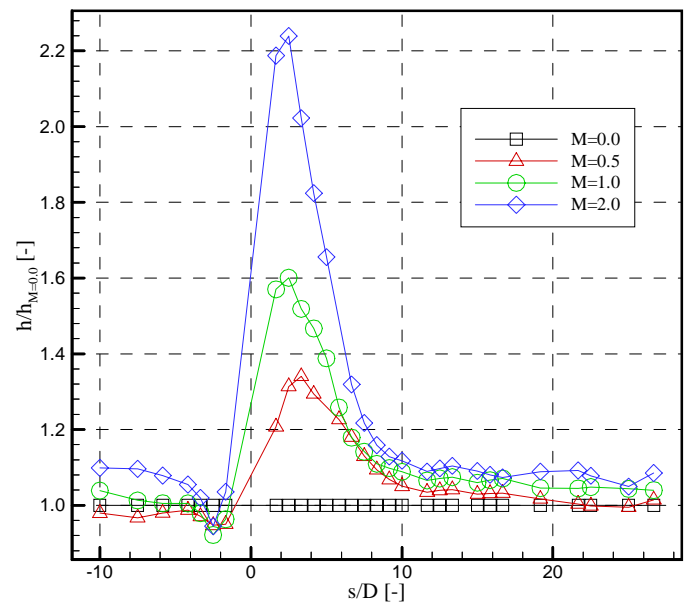
Fig. 15 Heat transfer coefficient referenced by M=0.0 ($\Delta T = T_w - T_{t,G}$)

The heat transfer coefficient distribution showed a significant influence by varying the blowing ratio upstream and downstream of the injection location. A comparison with the TLC measurements showed that some of the observed

7

phenomena could be detected in both measurements. Nevertheless, noticeable differences between the results of the two measurement techniques especially for the case without injection (M=0.0) could be observed. This led to different levels for the results referenced by the blowing ratio M=0.0. But in the vicinity of the hole a similar increase was detected. Another comparison with a flat plate investigation showed a better agreement for the referenced values further downstream.

In order to get a better comparability between the TLC and the hot-film results a measurement without film cooling holes is in progress.
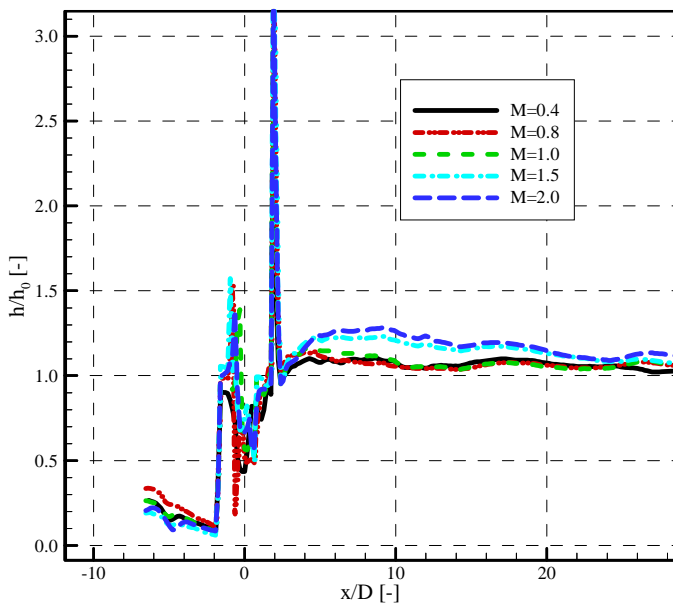
Fig. 16 Heat transfer coefficient referenced by M=0.0 (Baldauf [7])

ACKNOWLEDGMENTS

REFERENCES

1. Goldstein, R. J., 1971, "Film Cooling", Advances in Heat Transfer, Vol. 7, eds. Hartnett, J. P., Irving, T. F., Academic Press
2. Hippensteele, S. A., Russell, L. M., Stepka, F. S., 1981, "Evaluation of a Method for Heat Transfer Measurements and Thermal Visualization Using a Composite of a Heater Element and Liquid Crystals", ASME 81-GT-93
3. Camci, C., Kuisoon, K., Hippensteele, S. A., 1991, "A New Hue Capturing Technique for the Quantitative Interpretation of Liquid Crystal Images Used in Convective Heat Transfer Studies", ASME 91-GT-122
4. Wang, Z., Ireland, P., T., Jones, T., V., 1993, "An Advanced Method for Processing Liquid Crystal Video Signals From Heat Transfer Experiments", ASME 93-GT-282
5. Gillespie, D., et al., 1994, "Detailed Measurements of the Local Heat Transfer Coefficient in the Entrance to Normal and Inclined Film Cooling Holes", ASME 94-GT-1
6. Gritsch, M., Schulz, A., Wittig, S., 1998, "Heat Transfer Coefficient Measurements of Film Cooling Holes with Expanded Exits", ASME 98-GT-28
7. Baldauf, S., Schulz, A., Wittig, S., 1999, "High Resolution Measurements of Local Heat Transfer Coefficients by Discrete Hole Film Cooling", ASME Paper 99-GT-43
8. Goldstein, R., J., Jin, P., Olson, R., L., 1998, "Film Cooling Effectiveness and Mass/Heat Transfer Coefficient Downstream of one Row of Discrete Holes", ASME 98-GT-174
9. Haslinger W., Hennecke D., K., 1996, "The Ammonia And Diazo Technique With Co2-Calibration for Highly Resolving And accurate Measurement Of Adiabatic Film Cooling Effectiveness With Application To a Row Of Holes", ASME 96-GT-438
10. Popp, O., et al., 2000, "Investigation of Heat Transfer in a film cooled Transonic Turbine Cascade, Part II: Unsteady Heat Transfer", ASME 2000-GT-203
11. Hilditch, M. A. et al., 1996, "Unsteady Measurements in an Axial Flow Turbine", AGARD CP NO. 571
12. Sieverding, C. H., et al., 1998, "Experimental Investigation of the Unsteady Rotor Aerodynamics and Heat Transfer of a Transonic Turbine Stage", Lecture Series of the VKI on Blade Row Interference
13. Ganzert, W., Fottner, L., 1999, "An Experimental Study on the Aerodynamics and Heat Transfer of a Suction Side Film Cooled Large Scale Turbine Cascade", ASME 99-GT-039
14. Haselbach, F., 1997, "Thermalhaushalt und Kalibration von Oberflächenheißfilmen und Heißfilmarrays", Fortschritt-Berichte VDI: Reihe 7 Nr. 326
15. Tiedemann, M., 2000, "High frequency blade surface temperature determination using surface mounted hotfilm gauges", to be presented at XVth Bi-Annual Symposium on Measuring Technique
16. Heselhaus, A., 1997, "Ein hybrides Verfahren zur gekoppelten Berechnung von Heißgasströmung und Materialtemperaturen am Beispiel gekühlter Turbinenschaufeln", Doctoral Thesis Rur-Universität Bochum
17. Sturm, W., Fottner , L., 1985, "The High-Speed Cascade Wind Tunnel of the German Armed Forces University Munich", 8th Symposium on Measuring Techniques in Transonic and Supersonic Flows in Cascades and Turbomachines
18. Brunner, S., Teusch, R., Stadtmüller, P., Fottner, L., 1998, "The Use of Simultaneous Surface Hot Film Anemometry to Investigate Unsteady Wake Induced Transition in Turbine and Compressor Cascades", 14th Symposium on Measuring Techniques
19. Bruun, H., 1995, "Hot-Wire Anemometry: Principles and Signal Analysis", Oxford University Press